Environmental Science and Pollution Research (2025) 32:657–676
https://doi.org/10.1007/s11356-024-35647-y

RESEARCH ARTICLE

An exploratory study of volatile and semi-volatile organic compounds in $PM_{2.5}$ atmospheric particles from an outdoor environment in Brazil

Josimar M. Batista[1] · Eduard F. Valenzuela[1] · Helvécio C. Menezes[1] · Zenilda L. Cardeal[1]

Received: 9 July 2024 / Accepted: 21 November 2024 / Published online: 19 December 2024

Abstract

The development of methods for determining volatile and semi-volatile organic compounds in public spaces has become necessary to identify potential health and environmental risks. This study presents a practical methodology for sampling, extracting, detecting, and identifying these compounds in a vehicular traffic region in Belo Horizonte, Brazil. The methodology uses direct-immersion solid phase microextraction (DI-SPME) and static headspace (SHS) to extract SVOCs/VOCs. Comprehensive time-of-flight gas chromatography mass spectrometry (GC×GC/Q-TOFMS) and gas chromatography coupled to mass spectrometry (GC/MS) were used to detect and identify compounds. The analysed samples, collected with a high-volume sampler (Hi-Vol) with quartz filters and in which particulate matter ($PM_{2.5}$) was retained, showed the presence of more than 200 compounds, both biogenic (natural origin) and anthropogenic (human origin). Regarding the distribution of chemical classes, aromatic compounds were predominantly found at 29.2%, followed by esters at 20.8%, non-aromatic hydrocarbons at 5.6%, and carboxylic acids at 9.4%. Static headspace gas chromatography (HS-GC) enabled the identification and quantification of 21 volatile compounds, including BETX, dichloromethane, chloroform, and naphthalene, which are currently regulated by the US Environmental Protection Agency (EPA).

Graphical abstract

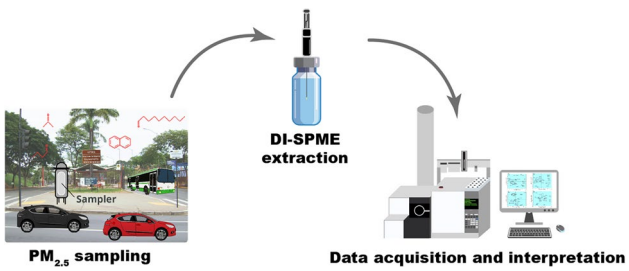

Keywords Air quality · DI-SPME-GC×GC-QTOFMS · HS-GC/MS · Semi-volatile organic compounds · Outdoor air analysis · Volatile organic compounds

Introduction

Volatile organic compounds (VOCs) have a boiling point between 50/100 °C and 240/260 °C, while semi-volatile organic compounds (SVOCs) have a boiling point range of 240/260 °C to 380/400 °C, measured at 101.3 kPa (EPA 2024). These groups of compounds consist primarily of carbon and hydrogen atoms (alkanes, olefins, aromatic hydrocarbons), but oxygen, nitrogen, sulphur, and halogen atoms

Responsible Editor: Gerhard Lammel

✉ Zenilda L. Cardeal
zenilda@ufmg.br

[1] Departamento de Química, ICEx, Universidade Federal de Minas Gerais, Avenida Antônio Carlos, Belo Horizonte, MG 6627, 370901, Brazil

(halogenated hydrocarbons) such as chlorine, bromine, and fluorine are also frequently found in their compositions.

SVOCs/VOCs are generated in various ways by natural sources and human activities. In human activities, SVOCs/VOCs are widely used in the footwear, steel, wood, cosmetics, and pharmaceutical industries through paints, solvent-based coatings, solvents, adhesives, dispersants, degreasers, and detergents. Evaporation, combustion, or transportation of these products is known to be an anthropogenic source (Dai et al. 2021). Many VOCs present in the atmosphere are of natural origin and are related to the decomposition processes of organic matter, such as methane (from ruminants), or are formed by vegetation, such as essential oils (biogenic volatile organic compounds, BVOCs), the ocean and volcanic activity (Li et al. 2020). Additionally, some VOCs originate from the consumer product sector, such as fragrances, skin creams, or cleaning products (Gerster et al. 2014).

Increased concentrations of SVOC/VOC in the air impact the environmental and health sectors. These compounds contribute to climate change, tropospheric ozone formation, and particulate matter ($PM_{2.5}$) (Guan et al. 2016; Li et al. 2023). This situation leads to respiratory problems such as acute lower respiratory tract infections (ALRTIs) (Lyu et al. 2020), chronic obstructive pulmonary disease (COPD) (Li and Ma 2021) as well as cardiovascular problems (Pathak and Viphavakit 2022), eye diseases (Yang et al. 2023) and negative impacts on agriculture (Wang et al. 2020). Certain SVOCs, such as polycyclic aromatic hydrocarbons, have been linked to mutations, male infertility (Kakavandi et al. 2023), and some cancers, such as lung cancer (LC) (Schmekel et al. 2014).

Destructive methods such as catalytic oxidation and biofiltration and recovery methods such as absorption, adsorption, condensation, and membrane separation have been developed to treat SVOCs/VOCs in air analysis (Zhu et al. 2020). Gas chromatography combined with mass spectrometry (GC/MS) is the applied technique for detecting and identifying SVOCs/VOCs (Lim et al. 2023). This technique offers many practical advantages, such as a large separation capacity, high sensitivity, and class chemical separation, mainly when an orthogonal second column is used (comprehensive two-dimensional gas chromatography, GC×GC) (Ieda and Hashimoto 2023). GC×GC with Q-TOF analyser is particularly advantageous for identifying many compounds at high resolution, allowing for the precise differentiation of individual substances in complex mixtures, which is essential for conducting comprehensive analyses in diverse environments.

There are several classical procedures for VOCs/SVOCs extraction and analysis, some of which commonly include thermal desorption (TD) (Kaikiti et al. 2022), liquid–liquid extraction (LLE) (Murrell and Dorman 2021), static headspace extraction (SHS) (Cardador and Gallego 2017), dynamic headspace extraction (DHS), also called purge trap (PT) (Moser et al. 2023), solid-phase extraction (SPE) (Liu et al. 2021), magnetic solid-phase extraction (MSPE) (Nie et al. 2016), and stir bar sportive extraction (León et al. 2006). The use of microextraction techniques, such as solid phase microextraction (SPME) (Martínez et al. 2022), needle trap device (NTD) (Jeong et al. 2024), liquid phase microextraction (LPME) (Sarafraz-Yazdi et al. 2008), and single-drop microextraction (SDME) (Delove Tegladza et al. 2020), has increased significantly in recent years for the analysis of SVOCs/VOCs. All these techniques have shown higher sensitivity, extraction efficiency, versatility, environmental friendliness, and selectivity than conventional methods (Jalili et al. 2019).

Traditionally, air sampling involves taking a representative sample volume using pumps that draw air and collect it in cylinders or sampling bags. These samples are then directly injected into the gas chromatograph for analysis. Although this approach is a good option for the analysis of indoor air, it is not recommended for the analysis of outdoor air, as obtaining a representative sample would require large sample volumes. In recent years, the analysis of particulate matter (PM), including $PM_{2.5}$ and PM_{10} (particles with aerodynamic diameters less than 2.5 and 10 µm, respectively), in outdoor air has been introduced as a more practical alternative (Murillo et al. 2017; Evagelopoulos et al. 2022). These atmospheric particles can originate from natural and anthropogenic sources and contain many chemical substances, including heavy metals and various volatile and semi-volatile organic compounds (Murillo et al. 2017; Maceira et al. 2020). In this way, the use of particulate filters in high-volume samplers enables analysis and a comprehensive understanding of the air we breathe.

The present study proposes the determination of SVOCs and VOCs in $PM_{2.5}$ samples collected in a vehicle traffic region in Brazil and analysed by direct-immersion solid-phase microextraction (DI-SPME) using GC×GC/Q-TOFMS. Furthermore, a complementary analysis was performed to quantify VOCs regulated by different environmental agencies, using HS-GC/MS, to identify potential exposure levels. The SVOC/VOC separation processes and multivariate statistical analysis were considered to optimise the parameters of GC×GC system, together with the validation of the analytical method HS-GC/MS.

Methodology

Chemicals and materials

Acetonitrile was purchased from J. T. Baker (New Jersey, USA), ultrapure water from Elga (Lane End, UK), HPLC

grade acetone from Merck (Darmstadt, Germany), and 70% alcohol solution from (CRQ, Brazil). Quartz filters (20.3 cm × 25.4 cm × 47 mm) were purchased from Whatman (Clifton, NJ, USA). SPME fiber made of polyacrylate (PA) (85 µm, 24 Ga, Fused Silica/SS) was purchased from Supelco (Bellefonte, EUA). SPME flasks (20 mL) were purchased from Filtrilo (Colombo, Brazil). Acquired analytical standards were described in the Supplementary Material (SM).

Sampling

The samples consisted of quartz fiber filters with retained $PM_{2.5}$ fraction and were collected in Belo Horizonte, Minas Gerais/Brazil, according to the methodology described by dos Santos et al. (2020). The sampling occurred between March 10 and April 7, 2022, on non-sequential days (an average of four collections per week). Two collection points were selected on the UFMG Pampulha campus: Antônio Carlos entrance (19°51′47.3″S 43°57′30.2″W), referred to as PAC (16 samples) in the rest of the text, located on Av. Antônio Carlos, with high vehicle traffic and Ecological Park (19°87′34.7″S, 43°97′24.8″W), abbreviated ECO (17 samples), with less vehicle traffic and rich vegetation. Filters were previously calcined in a muffle furnace at 450° C for 4 h. This pre-treatment had the function of removing organic contaminants and removing moisture from the filters. The filters were then stored in a silica gel desiccator for 24 h. Then, each one was sampled for 24 h in a high-volume (Hi-Vol) sampler (Energética, Rio de Janeiro, Brazil), using active sampling with a flow rate of 1.1 m^3 min^{-1}, totaling 1584 m^3 of air sampled per filter.

Solid phase microextraction

The filter samples were extracted by DI-SPME, according to a procedure adapted from dos Santos et al. (2020) and Valenzuela et al. (2020), using polyacrylate (PA) as a coating fibre. Each filter containing PM was divided into 6 mm diameter circles, using a hole puncher, taken from homogeneously distributed regions on the filter surface. The six circles of each sample were placed in a glass flask, to which 150.0 µL of acetonitrile was added, and the volume was increased to 20.0 mL with ultrapure water. Acetonitrile had the function of changing the polarity of the medium. Pure water has a high polarity, which would hinder the solubilisation of the less polar compounds and, consequently, the partition of the compounds between the medium and the SPME fiber. Each vial contained one sample, totaling 33 samples analysed. Manual SPME extraction was performed for 45 min under magnetic stirring (250 rpm) and heating at 70 °C. Subsequently, the SPME fiber was exposed in the GC×GC injector system for 3 min at 250 °C with 1 min of desorption (2 min was added to the fiber cleaning).

Quality control

After the treatment in the muffle furnace, the filters were individually packed in hermetically sealed bags (aluminium coated) to avoid cross-contamination. All procedures were performed with clean nitrile gloves on cleaned benches with a 70% ethyl alcohol solution, using plastic tweezers to manipulate filters. The hole puncher was cleaned with HPLC acetone between one filter and another. Furthermore, the SPME fiber was preconditioned to eliminate interferents in a dedicated SPME oven (270 °C for 2 min), with subsequent blank analysis to confirm that the fiber was suitable for extraction. A matrix blanks (non-sampled filters) analysis and the SPME extraction solvent blanks were performed to verify the background interferences (Fig. S2 and S3). The blank analysis followed the same extraction and chromatographic procedures.

GC×GC/Q-TOFMS analysis

The untargeted determination of the compounds contained in the particulate matter samples was carried out using GC×GC. The equipment used was a gas chromatograph (Agilent, model 7890B) coupled to a mass spectrometer with a hybrid quadrupole time of flight analyser (Q-TOFMS/MS, Agilent, model 7250) made in Wilmington (DE, US), equipped with the NIST 17 Mass Spectra Library, version 2.3 (2017). In the GC×GC system, a thermal loop modulator (Zoex, model ZX2) made in Houston (TX, USA) was used. GC Image software (version 2.9r2 GC×GC-HRMS) was used to acquire and process the colour plots (two-dimensional chromatograms).

The chromatograph injector operated at 250 °C in splitless mode for 1 min. The first dimension ^1D column was HP-5MS (30 m × 250 µm × 0.25 µm), and the second dimension ^2D column was Rxi-17Sil MS (2 m × 0.15 mm × 0.15 µm). Helium was a carrier gas in the 1.0 mL min^{-1} flow. The oven started at 50 °C, then increased to 150 °C at 20 °C min^{-1}, then up to 180 °C (1 min), at 3 °C min^{-1}, and then up to 280 °C (2 min) at 7 °C min^{-1}. The transfer line operated at 280 °C, the ionisation source at 200 °C, and the quadrupole at 150 °C. The ionisation was performed by electron ionisation (EI) in positive mode at 70 eV, and MS operated in full scan mode, sweeping the ion band from *m/z* 50 to *m/z* 550. The TOF operated at an acquisition rate of 50 Hz, and the detector voltage was 800 V for the microchannel plate (MCP) and 551 V for the photomultiplier tube (PMT). The temperature of the cold jet was −80 °C.

The parameters affecting the modulation process were optimised through the Design of Experiments (DoE) and

Response Surface Methodology (RSM) using a filter sample, and the results were: + 30 °C for the hot jet temperature offset, a hot jet duration of 393 ms, a cold jet flow rate of 12.5 L min^{-1}, and a modulation period of 6 s.

Design of experiments and optimisation of the response surface methodology

The choice of modulation parameters is crucial for good two-dimensional separation. However, combining the parameters is difficult as many variables must be controlled simultaneously. Therefore, DoE in selecting parameters that affect modulation and RSM in optimising important parameters is very useful in reducing the number of experiments and achieving the best combination of parameters. Many studies have used DoE and RSM in the optimisation of two-dimensional chromatographic separation parameters, including modulation (Gaines 1998; Skartland et al. 2011; Stefanuto et al. 2017; Kulsing et al. 2020; Zou et al. 2021; Boegelsack et al. 2021; Vyviurska et al. 2022) and as in the optimisation of extraction procedures used in GC×GC (Cheong et al. 2011; Salvador et al. 2013; Setyaningsih et al. 2019; Drabińska and Jeleń 2022; Bhatt et al. 2022). However, no studies were found that optimised modulation parameters for analysing VOCs/SVOCs in atmospheric particulate matter. Therefore, an investigation in this sense is proposed in this paper using a fractional factorial design, as DoE, and Doehlert matrix as RSM. Doehlert design is a modeling technique widespread in optimisation procedures. This model is based on the arrangement of data in polygons (e.g., triangular face, square face, and the apex of the cuboctahedron) surrounding a central point, indicating the optimal region (Cerqueira et al. 2021). A fractional factorial design has the advantage of requiring fewer experiments than a complete factorial design. In the same sense, the Doehlert matrix provides optimisation results like those of other methods, such as Box-Behnken and Central Composite, but with a much smaller number of experiments than required to build these other optimisation models.

A two-level fractional factorial design, with resolution IV (2^{4-1}_{IV}) and three central points, was constructed to select significant variables and comprise 11 experiments (Table S1). From the fractional factorial experimental design results analysis, the cold jet flow, and the hot jet duration (with three central points) were selected as variables for the Doehlert matrix (Table S2).

Data processing

The two-dimensional chromatograms were processed with the software GC Image, version 2.9r1 GC×GC. Baseline correction of all chromatograms was performed first using the MS data channel, with a median mean filter, five deadband data points, a distribution equal to 7, a filter window size equal to 7, and 1 stride per modulation cycle. The MS data were divided into integer intervals with the rounding parameter for the integer mass equal to 0.5. Subsequently, all plots were aligned with the mass spectra and retention times ${}^{1}t_R$ and ${}^{2}t_R$, with $\Delta^{1}t_R$ %RSD < 3.03% and $\Delta^{2}t_R$ %RSD < 4.84%. After pre-processing, an attempt was made to identify the compounds.

The aligned data were imported into the MATLAB software, version R2010a, as a matrix containing the samples in the rows and the peak intensity of the identified compounds in the columns. This data set was used to build a PCA (principal component analysis) model using the PLS Toolbox, version 5.2.2. The pre-processing used for the PCA model was mean centering. Samples with abnormal values of Q residual and Hotelling T^2 (outliers) were removed.

Compounds identification attempt

The attempt to identify the compounds present in the PM was made by automatical comparison of the raw spectra with the NIST 17 library, using MS peak signal-to-noise ratio (S/N) > 500 and a match factor ≥ 750. The confirmation of compounds identified was performed manually by linear retention indexes (I) comparison with $\Delta I_{error} \leq 3\%$. The retention indexes were calculated according to the methodology developed by van Den Dool and Kratz (1963) and searched in NIST web book database (NIST 2017).

HS-GC/MS analysis

The full methodology and method validation for extraction through static headspace are presented in the SM. The methodology was developed considering 67 VOCs regulated by environmental agencies such as EPA and the *Conselho Nacional do Meio Ambiente (CONAMA)* in Brazil.

Results and discussion

Thermal modulation process optimisation

Untargeted analyses require chromatographic methods capable of detecting the maximum number of compounds in the sample with the best resolution. In GC×GC, the "heart" of the system is the modulator. Therefore, optimising the modulation parameter is crucial to comprehensively analysing the total compounds.

A quartz filter sample from the PAC set was used for the optimisation experiments. Replicates were performed at the central point to assess the model's lack of fit. The number of peaks with a resolution (R_s) > 1.2 and SNR > 500

was chosen as the combined response (R). The response was normalised by square root, and the residuals showed homoscedasticity. The effects that were significant in the fractional factorial design were cold jet flow (f_{cj}), hot jet duration (t_{hj}), and modulation period (P_M), as shown in the Pareto diagram (Fig. 1). Analysis of variance (ANOVA) for the selected factorial model shows that the regression was significant ($p < 0.05$), non-significant for lack of fit ($p > 0.05$), and sufficient fit ($R^2 = 0.9323$). The equation related to the factors was then $R = 9.52 + 0.46P_M - 0.03 t_{hj} - 0.27f_{cj}$.

Figure 2a–e shows the variations of the factors in the responses. Higher values for the modulation period increase the response (Fig. 2a). This can be explained by the prolonged contact time of the analytes with the second-dimension column, which can increase to enhance the number of peaks with higher resolution. Lower values for the duration of the hot jet (Fig. 2b) showed an increased response. Since most of the analytes that make up the sample do not have high boiling temperatures, a very long hot jet pulse is not required to efficiently release the analytes from the loop in the ^2D column. High hot-jet pulse values can lead to volatility losses for these compounds. Lower values for cold jet flux (Fig. 2c) also increased the response, indicating that no long cold jet time is required for compounds focusing on the modulator (Snow 2020).

Based on the Pareto diagram of the factorial design (Fig. 1), the duration of the hot and cold jet flow was the two factors that most influenced the response, so they were selected for optimisation using the Doehlert matrix. The modulation period was set to 6 s, and the offset of the hot jet was set to + 30 °C (non-significant variable). The response chosen for the construction of the model was the same as that of the factorial design. A quadratic model was fitted to the experimental data, with $R^2 = 0.9915$. The terms of the model were statistically significant ($p < 0.05$), and there was no lack of fit ($p > 0.05$). Furthermore, the model was fit for prediction, with a difference of less than 0.2 between the predicted R^2 and the adjusted R^2. The residuals showed a homogeneous distribution, and no outliers were detected. Thus, the final equation of the model in terms of the statistically significant factors was $R = -27.9768 + 0.2461t_{hj} + 9.2258f_{cj} + 0.0058t_{hj}f_{cj} - 0.0004{t_{hj}}^2 - 0.4566{f_{cj}}^2$. The response surface of the fitted model is shown in Fig. 2f.

The optimal region (with maximal number of peaks, N, with $R_s > 1.2$ and SNR > 500) of the response surface

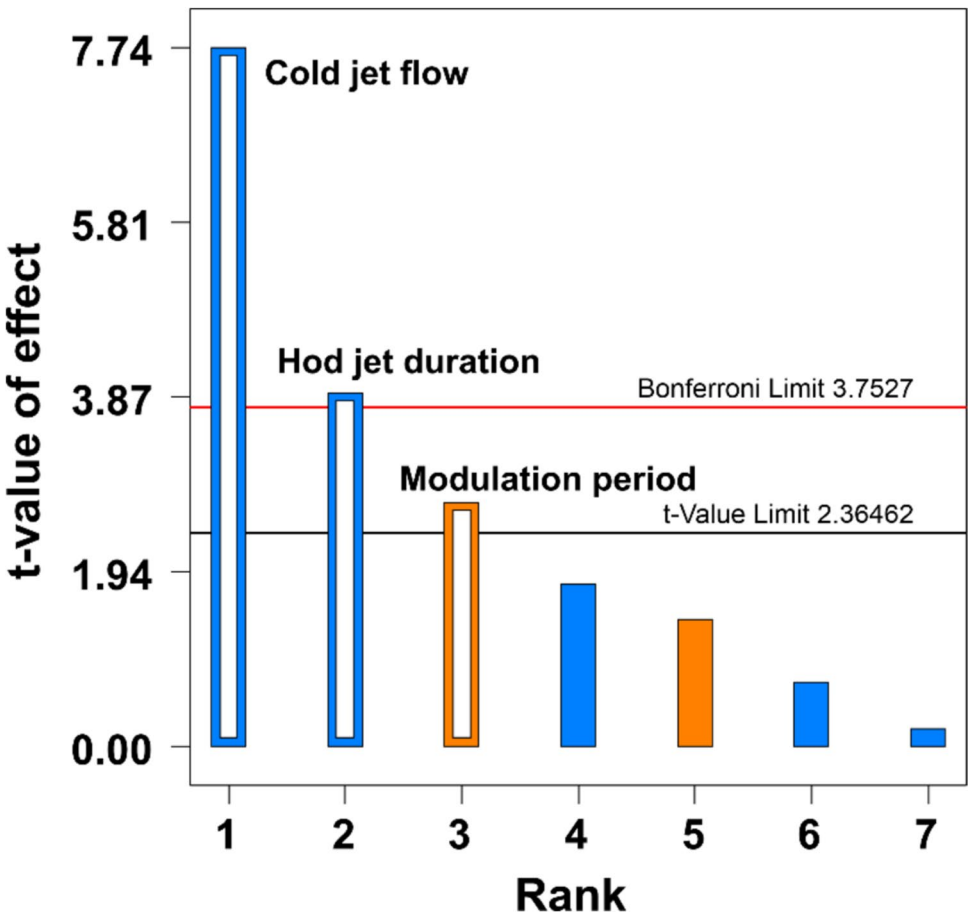

Fig. 1 Pareto chart with the significant effects of the fractional factorial design

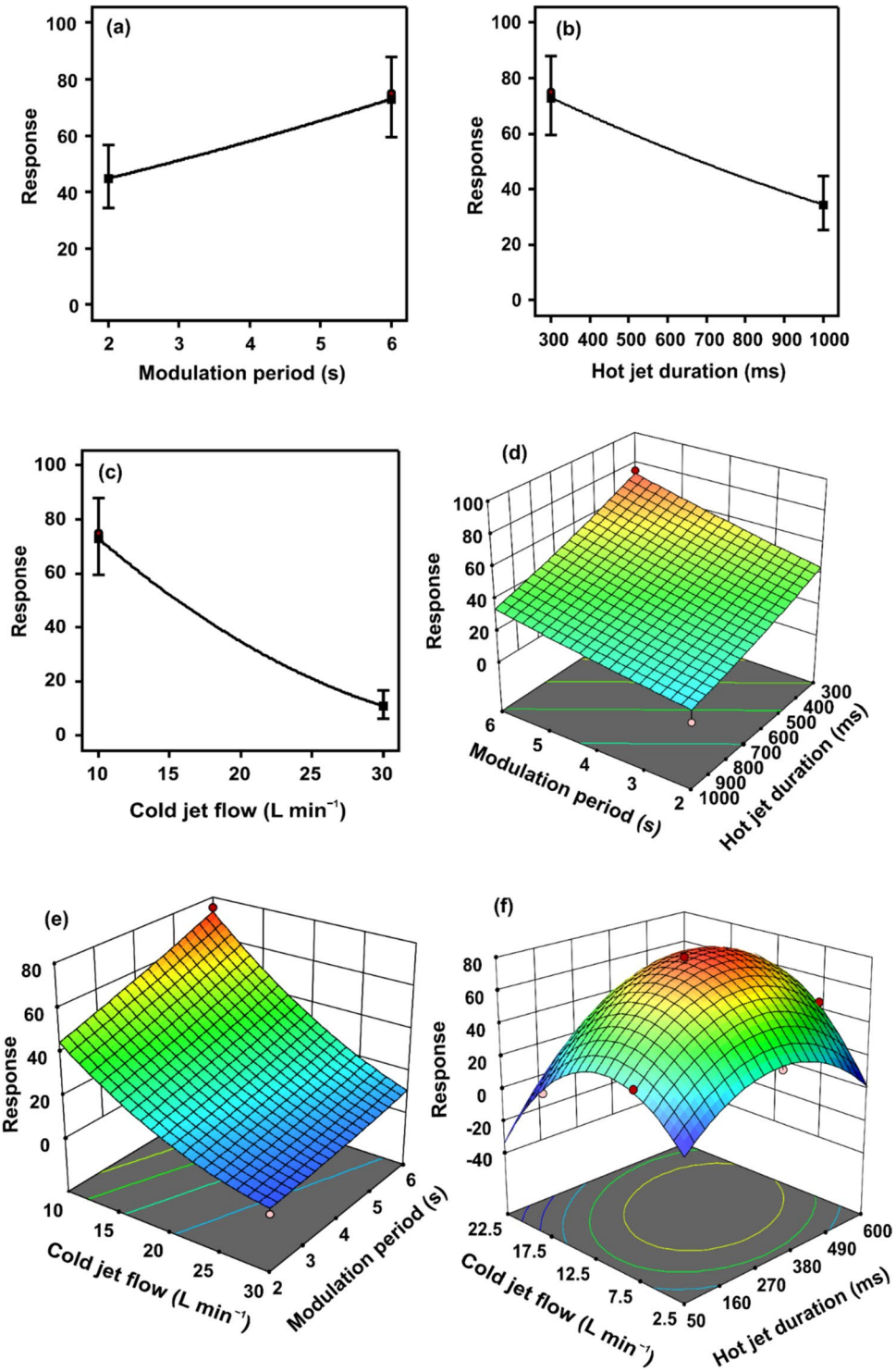

Fig. 2 Optimisation graphical results: **a** influence of the modulation period in the factorial response; **b** influence of the hot jet duration in the factorial response; **c** influence of the cold jet flow in the factorial response; **d**, **e** response surfaces for the factorial design; **f** response surface for the Doehlert matrix design with P_M fixed in 6 s

(red colour, $75 < N < 80$) shows that the optimal conditions were 393 ms hot jet flow and cold jet flow of 12.5 L min^{-1}. These conditions were applied to analyse some filter samples, and the response was within the optimal range. Therefore, the optimised conditions were applied to analyse all filter samples.

Multivariate analysis

A total of 189 VOCs and SVOCs were identified in the samples (Table 1), and the representative chromatograms are shown in Fig. S1. The heat map showing the distribution of compounds by sampling point is shown in Fig. 3.

Table 1 Probable identification of compounds found in all $PM_{2.5}$ samples, with compared retention data

N°	Compound	CAS number	^1t_R (min)	^2t_R (s)	Calculated[1] *I*	Literature *I*
1	4-Nitro-2H-benzotriazole	6299–39-4	5.70	1.93	920	-
2	3-Amino-7-nitro-1,2,4-benzotriazine 1-oxide	-	5.70	4.87	920	-
3	Fumaronitrile	764–42-1	6.00	4.99	980	917
4	(4-Hydroxyphenyl)phosphonic acid	33795–18-5	6.60	1.89	1100	-
5	Pentadecafluorooctanoic acid, 2-ethylhexyl ester	-	6.80	1.91	1129	1145
6	2-Bromo-4,6-difluoroaniline	444–14-4	7.20	3.04	1186	1262
7	Decanal	112–31-2	7.40	1.95	1213	1206
8	2,5-Furandione, 3-(1,1-dimethylethyl)-	18261–07–9	7.50	1.93	1225	1282
9	2-(6-Methoxypyridin-3-yl)ethanamine	579515–25-6	8.20	2.11	1309	1319
10	Oxirane, decyl-	2855–19-8	8.30	2.03	1318	1307
11	10-Undecen-1-ol	112–43-6	8.40	1.93	1327	1347
12	Benzene, 1-isocyanato-2-methoxy-	700–87-8	8.50	2.09	1336	-
13	Benzaldehyde, 2-hydroxy-4-methoxy-	673–22-3	8.60	2.94	1345	1348
14	4,6-Dimethylpyridine-3-carboxylic acid	22047–86-5	8.90	1.83	1373	1370
15	n-Decanoic acid	334–48-5	9.00	2.01	1382	1373
16	1-Tetradecene	1120–36-1	9.20	2.01	1400	1392
17	Pyrrole, 2-methyl-5-phenyl-	3042–21-5	9.30	5.37	1408	1462
18	Dodecanal	112–54-9	9.40	2.11	1417	1409
19	1,9-Nonanediol	3937–56-2	9.40	2.01	1417	1416
20	1H-Indene-1-methanol, α-methyl-, acetate	51926–98-8	9.50	2.35	1425	1491
21	1-Adamantyl methyl ketone	1660–04-4	9.80	0.68	1450	1462
22	Benzoic acid, 4-formyl-	619–66-9	10.00	2.51	1467	1452
23	Undecanoic acid	112–37-8	10.10	2.09	1475	1475
24	Ethanone, 1-(2,3-dihydro-1H-inden-5-yl)-	4228–10-8	10.30	2.37	1492	1546
25	1-Pentadecene	13360–61-7	10.40	2.07	1500	1492
26	Methyl hydrogen phthalate	4376–18-5	10.50	2.58	1506	1530
27	Undecanoic acid, ethyl ester	627–90-7	10.50	2.19	1506	1494
28	1,4-Benzenedicarboxaldehyde, 2,5-dimethyl-	7044–92-0	10.50	2.39	1506	1510
29	2,4-Dimethoxyamphetamine	23690–13-3	10.60	2.60	1513	1550
30	1-Pentadecyne	765–13-9	10.70	2.13	1519	1518
31	Dimethylsulfoxonium formylmethylide	-	10.80	1.77	1525	-
32	Vanillin, acetate	881–68-5	10.80	2.68	1525	1536
33	Propiophenone, 2,2′,4′,6′-tetramethyl-	2040–22-4	11.30	2.76	1556	1503
34	1H-Pyrazole, 3-methyl-5-phenyl-	3347–62-4	11.50	2.66	1569	1584
35	2-Naphthalenamine, N-methyl-	2216–67-3	11.60	2.76	1575	1543
36	1,10-Dichlorodecane	2162–98-3	11.70	2.23	1581	1536
37	n-Tridecan-1-ol	26248–42-0	11.70	2.19	1581	1577
38	Cetene	629–73-2	12.00	2.05	1600	1592
39	1 s,4R,7R,11R-1,3,4,7 Tetramethyltricyclo[5.3.1.0(4,11)]undec-2-en-8-one	-	12.00	2.29	1600	1587
40	2(3H)-Benzoxazolone, 3-(hydroxymethyl)-	-	12.10	1.49	1605	1628
41	1-Propanamine, 3-dibenzo[b,e]thiepin-11(6H)-ylidene-N,N-dimethyl-, S-oxide	1447–71-8	12.20	2.09	1610	-
42	Tetradecanal	124–25-4	12.30	2.27	1615	1613
43	Phenol, 3,5-bis(1,1-dimethylethyl)-	1138–52-9	12.40	2.41	1620	1555
44	Phthalamic acid	88–97-1	12.60	3.08	1630	1673
45	S(-)-Methcathinone	112117–24-5	12.90	1.81	1645	1632
46	N-ethyl-2,3-methylenedioxyphenethylamine	-	13.10	2.76	1655	1634
47	Tridecanoic acid	638–53-9	13.20	2.35	1660	1666
48	Tridecane, 1-bromo-	765–09-3	13.30	2.39	1665	1651
49	3-Trifluoromethylbenzoic acid, 2-octyl ester	-	13.60	2.41	1680	1680

Table 1 (continued)

N°	Compound	CAS number	$^{1}t_R$ (min)	$^{2}t_R$ (s)	Calculated[1] *I*	Literature *I*
50	3-Trifluoromethylbenzoic acid, 2-octyl ester	-	13.60	3.88	1680	1639
51	Aniline, N-methyl-N-(2,2,2-trichloroethoxycarbonyl)-	62–53-3	13.70	1.79	1685	1696
52	1-Heptadecene	6765–39-5	13.90	2.15	1695	1692
53	2,6-Difluoro-3-methylbenzoic acid, hexyl ester	-	14.00	3.80	1700	1698
54	Propanoic acid, 2-methyl-, 2-ethyl-1-propyl-1,3-propanediyl ester	-	14.10	2.37	1704	1690
55	Pentadecanal	2765–11-9	14.30	2.39	1713	1715
56	Chloroacetic acid, 10-undecenyl ester	79–11-8	14.70	2.33	1730	1696
57	1-Phenyl-2-(2-pyridyl)ethanedione	13474–48-1	15.00	3.34	1743	1832
58	Succinic acid, 2,3-dichlorophenyl 2,2,3,3,3-pentafluoropropyl ester	-	15.00	2.43	1743	1780
59	Benzophenone dimethyl ketal	2235–01-0	15.10	3.44	1748	1733
60	Diethylene glycol adipate	58984–19-3	15.10	3.54	1748	1858
61	1,3-Dioxolane-2,2-dipropanoic acid, diethyl ester	19719–88-1	15.20	3.64	1752	1842
62	2-Trifluoromethylbenzoic acid, 2-methyl ester	433–97-6	15.20	6.02	1752	1767
63	Sulfurous acid, nonyl 2-propyl ester	-	15.30	2.25	1757	1773
64	Isocitronellol	18479–52-2	15.40	2.94	1761	1854
65	Hexanoic acid, 3,5,5-trimethyl-, octyl ester	-	15.40	2.39	1761	1737
66	4-Pentadecyne, 15-chloro-	56554–70-2	15.80	2.45	1778	1755
67	Carbonic acid, dodecyl ethyl	35108–03-3	15.80	2.35	1778	1755
68	4,6,6-Trimethyl-7-morpholino-1,4-oxazepane	76503–76-9	15.80	2.47	1778	1739
69	Cyclopentanecarboxylic acid, 3-methylene-, 1,7,7-trimethylbicyclo[2.2.1] hept-2-yl ester	-	15.90	2.74	1783	1785
70	3-Octadecene, (E)-	-	16.10	2.23	1791	1785
71	1,4-Benzenediol, 2,5-bis(1,1-dimethylethyl)-	-	16.20	2.49	1796	1823
72	Tetradecane, 1-iodo-	19218–94-1	16.30	2.19	1800	1827
73	Heptadecane, 2,6-dimethyl-	54105–67-8	16.50	2.23	1808	1782
74	E-11(13-Methyl)tetradecen-1-ol acetate	-	16.70	2.58	1815	1822
75	Heptadecanal	629–90-3	16.70	2.47	1815	1899
76	Benzoic acid, octyl ester	94–50-8	16.80	2.82	1819	1792
77	Disulfide, bis(1,1,3,3-tetramethylbutyl)		16.90	2.37	1823	1775
78	1-(7-Methyl-4,8-diphenyl-pyrazolo[5,1-c][1,2,4]triazin-3-yl)-ethanone	-	17.10	3.04	1831	-
79	Naphthalene, 2,7-bis(1,1-dimethylethyl)−1,2,3,4-tetrahydro-	-	17.30	2.70	1838	1768
80	Oxalic acid, isobutyl nonyl ester	959275–48-0	17.40	2.31	1842	1783
81	2-Methoxy-2′-methyl-stilbene	-	17.60	3.28	1850	1876
82	Pentadecanoic acid	1002–84-2	17.80	2.64	1858	1867
83	1,2,4-Benzenetricarboxylic acid, 1,2-dimethyl ester	54699–35-3	17.90	2.52	1862	1910
84	Methyl 4-bromo-5-phenylisoxazole-3-carboxylate	-	18.10	1.79	1869	1896
85	Hexadecanal, 2-methyl-	55019–46-0	18.10	2.39	1869	1835
86	4-tert-Butyl-2,6-diisopropylphenyl acetate	-	18.20	3.16	1873	1883
87	1-Naphthol, 1,2,3,4-tetrahydro-2-(methylsulfonyl)-	-	18.80	3.56	1896	1922
88	5-Octadecene, (E)-	18899–24-6	18.80	2.39	1896	1818
89	5-(Phenylsulphonyl)dihydro-1,3,5-dioxazine	-	18.80	3.84	1896	1891
90	Nonadecane	629–92-5	18.90	2.23	1900	1900
91	2-Heptadecanone	2922–51-2	19.00	2.60	1904	1904
92	2-Pentyl methylphosphonofluoridate	-	19.10	3.24	1909	-
93	5-(2,4-Dimethyl-phenyl)−2H-pyrazol-3-ol	-	19.10	3.80	1909	1850
94	Sulfurous acid, 2-ethylhexyl isohexyl ester	-	19.20	2.29	1913	1908
95	Salicylic acid, 2-methylbutyl ether, 2-methylbutyl ester	-	19.20	2.70	1913	1929
96	1,14-Tetradecanediol	19812–64-7	19.40	2.58	1922	1924
97	Benzoic acid, 2-phenoxy-	2243–42-7	19.40	3.50	1922	1913
98	3,5-di-tert-Butyl-4-hydroxyacetophenone	14035–33-7	19.60	3.04	1930	1903

Table 1 (continued)

N°	Compound	CAS number	$^{1}t_R$ (min)	$^{2}t_R$ (s)	Calculated[1] *I*	Literature *I*
99	1,2-Naphthalenedione, 3,8-dimethyl-5-(1-methylethyl)-	5574–34-5	19.90	2.66	1943	1942
100	Anthracene, 9-ethyl-1,2,3,4,5,6,7,8-octahydro-	-	19.90	2.56	1943	1865
101	2,15-Hexadecanedione	18650–13-0	20.10	2.49	1952	1884
102	Bis[(2-chlorocyclopentyl)methyloxy]methane	-	20.30	2.13	1961	2007
103	Palmitic acid	57–10-3	20.40	2.47	1965	1968
104	1,9-Bis(formamido)nonane	-	20.40	2.82	1965	1888
105	Caffeine	58–08-2	20.40	4.08	1965	1835
106	Phthalic acid, isobutyl 2-pentyl ester	-	20.70	3.40	1978	2008
107	Dibutyl phthalate	84–74-2	20.70	3.02	1978	1965
108	N-[[2-Morpholino]ethyl]succinamic acid	-	20.90	4.16	1987	2075
109	Acetamide, N-(5-methylisoxazol-3-yl)−2-morpholin-4-yl-	-	20.90	2.43	1987	1970
110	Propan-1-ol, 1-ethyl-1-phenyl-3-(1-piperidyl)-	6853–22-1	21.00	4.79	1991	1995
111	Oxamide, N-(2-morpholinoethyl)-	-	21.00	2.52	1991	1929
112	9-Phenanthrenecarbonitrile, 9,10-dihydro-	56666–55-8	21.00	3.62	1991	1920
113	Eicosane	112–95-8	21.10	2.23	1996	2000
114	3,3,5-Trimethylcyclohexyl 2-acetoxybenzoate	-	21.10	2.66	1996	2047
115	Heptadecanenitrile	5399–02-0	21.30	2.49	2005	1956
116	4,5-Dimethyl-4-nitro-2-phenyl-2,4-dihydro-pyrazol-3-one	-	21.40	2.74	2010	2020
117	Acetohydrazide, 2-hydroxy-2-phenyl-N2-but-2-enylideno-	-	21.50	1.01	2015	2077
118	9-Eicosyne	71899–38-2	21.70	2.35	2025	2027
119	Hexadecane, 1-iodo-	544–77-4	21.80	2.17	2030	2038
120	Coumarin-6-ol, 3,4-dihydro-4,4,5,7-tetramethyl-	-	21.80	2.78	2030	1974
121	Heptadecanoic acid, methyl ester	1731–92-6	21.90	2.43	2035	2028
122	Palmitoleic acid	373–49-9	22.10	2.43	2045	1951
123	Pyracarbolid	24691–76-7	22.10	3.72	2045	1943
124	2,4′-Dichloro-4-methoxydiphenyl ether	-	22.20	2.27	2050	1992
125	Benzamide, N-(tetrahydro-4-oxo-3-thienyl)-	62578–77-2	22.50	1.87	2065	2046
126	Propanedinitrile, cyclohexyl(2-methylcyclohexyl)-	74764–55-9	22.50	5.59	2065	2106
127	Heptadecanoic acid	506–12-7	22.50	2.45	2065	2071
128	Heneicosane	629–94-7	23.30	2.19	2106	2100
129	Stearic acid	57–11-4	23.60	2.29	2124	2153
130	2,3,3′,4-Tetrachloro-1,1′-biphenyl	41464–43-1	23.60	2.82	2124	2109
131	Hexadecanoic acid, 2-methylpropyl ester	110–34-9	23.70	2.33	2129	2135
132	1,16-Hexadecanediol	7735–42-4	23.70	2.39	2129	2130
133	9,10-Dimethylanthracene	781–43-1	23.80	3.20	2135	2136
134	Oleic acid	112–80-1	24.00	4.81	2147	2141
135	2-(5-Chloro-1H-1,2,4-triazol-3-yl)benzoic acid	-	24.20	3.50	2159	2144
136	Phthalic acid, 2-methylbutyl pentyl ester	-	24.50	2.64	2176	2171
137	Benzene, 1,1′-(1,3-butadiyne-1,4-diyl)bis-	886–66-8	24.60	3.38	2182	2142
138	Acridin-9-amine, 1,2,3,4-tetrahydro-5,8-dimethyl-	-	24.70	3.06	2188	2249
139	1-Docosene	1599–67-3	24.70	2.39	2188	2193
140	cis-13-Octadecenoic acid	13126–39-1	24.70	2.90	2188	2179
141	1-Morpolino-2,3-butadiene	-	24.80	2.31	2194	-
142	Sulfurous acid, butyl undecyl ester	-	25.00	2.19	2207	2235
143	Oxalic acid, dodecyl isohexyl ester	-	25.10	2.66	2213	2280
144	Nonadecanoic acid, methyl ester	1731–94-8	25.40	2.35	2233	2228
145	1H-Phenanthro[9,10-c]pyrazole	-	25.60	3.24	2247	2275
146	cis-10-Nonadecenoic acid	73033–09-7	25.60	2.35	2247	2256
147	2H-Pyran-2-one, tetrahydro-6-tridecyl-	1227–51-6	25.60	2.62	2247	2199
148	5-Methyl-Z-5-docosene	-	25.70	2.70	2253	2292

Table 1 (continued)

N°	Compound	CAS number	$^{1}t_R$ (min)	$^{2}t_R$ (s)	Calculated[1] *I*	Literature *I*
149	Pentadecanamide, 15-bromo-	-	26.20	2.54	2287	2218
150	Sulfurous acid, butyl tridecyl ester	959067–51-7	26.50	2.19	2307	2334
151	Pyrene, 2-methyl-	3442–78-2	26.50	3.26	2307	2254
152	Benzamide, 4-ethyl-N-(2-ethylphenyl)-	-	26.80	1.91	2329	2292
153	2-Anilino-4,6-di-tert-butylphenol	-	26.90	3.68	2336	2440
154	Cyclohexane, (1-octylnonyl)-	55124–77-1	26.90	2.35	2336	2307
155	Fumaric acid, 2-ethylhexyl octyl ester	-	26.90	2.25	2336	2288
156	Phenanthrene, 2,4,5,7-tetramethyl-	7396–38-5	27.00	3.00	2343	2235
157	1,3,5-Triazine-2,4,6-triamine, N-(4-methylphenyl)-	-	27.30	3.36	2364	2284
158	D-Mannopentadecane-1,2,3,4,5-pentaol	-	27.70	0.26	2393	2404
159	Tetracosane	646–31-1	27.80	2.11	2400	2400
160	Kaur-16-en-18-ol, (4α)-	-	27.90	2.90	2408	2400
161	5-Methoxy-[1,2,3]oxadiazole	-	27.90	2.29	2408	-
162	Benzoic acid, 2,4-dichloro-, 4-acetylphenyl ester	-	28.20	3.76	2431	2342
163	Benzoic acid, 2,6-dichloro-, 2-acetylphenyl ester	-	28.20	2.90	2431	2342
163	Heneicosanoic acid, methyl ester	6064–90-0	28.30	2.33	2438	2429
165	Sulfurous acid, pentadecyl 2-propyl ester	-	28.40	2.19	2446	2370
166	Arachidic acid	506–30-9	28.40	2.07	2446	2564
167	Heneicosanoic acid	2363–71-5	28.60	2.07	2462	2463
168	trans-8,9-Dihydro-11-methylbenz(a)anthracene-8,9-diol	83462–60-6	28.70	3.28	2469	2593
169	Dodecanoylhydrazide, N2-(1-methylpentylideno)-	-	28.70	2.84	2469	2403
170	Oleamide	301–02-0	28.70	2.58	2469	2397
171	Sulfurous acid, butyl tetradecyl ester	-	29.10	2.11	2500	2434
172	2,2′-Bibenzimidazole	14468–52-1	29.20	3.50	2508	2502
173	2H-1-Benzopyran, 2,2-diphenyl-	4222–08-6	29.20	3.10	2508	2419
173	p-Cyanophenyl p-(2-propoxyethoxy)benzoate	-	30.00	0.76	2575	2574
175	Di-n-decylsulfone	500026–38-0	30.0	2.23	2575	2516
176	Sulfurous acid, octadecyl 2-propyl ester	-	30.70	2.13	2636	2668
177	4-Trifluoromethylbenzoic acid. heptadecyl ester	-	30.70	2.51	2636	2598
178	Heptacosane	593–49-7	31.40	2.17	2700	2700
179	Succinic acid, 4-chloro-3-methylphenyl 2-methoxyphenyl ester	-	31.80	5.59	2736	2745
180	Cyclodocosane, ethyl-	296–86-6	31.90	2.31	2745	2798
181	4,4′-bi-4H-pyran, 2,2′,6,6′-tetrakis(1,1-dimethylethyl)−4,4′-dimethyl-	-	32.00	5.49	2755	2608
182	Sulfurous acid, butyl heptadecyl ester	-	32.10	2.15	2764	2732
183	7-Hydroxybenzo[b]thiophene-3-carboxylic acid, 2-acetylamino-6-dimethylaminomethyl-, ethyl ester	-	32.40	3.84	2791	2796
184	Quinoline, 4-(2-hydroxy-2-methoxy-1-thioxoethyl)−2-phenyl-	-	32.4	3.02	2791	2848
185	Octacosane	630–02–4	32.0	2.21	2800	2800
186	Terephthalic acid, 2-ethylhexyl octyl ester	-	33.10	3.04	2855	2768
187	Terephthalic acid, 6-methylhept-2-yl octyl ester	-	33.10	2.60	2855	2860
188	Octacosane, 2-methyl	1560–98-1	33.20	2.25	2864	2859
189	Sulfurous acid, butyl octadecyl ester	-	33.30	2.37	2873	2831

[1]t_R is the retention time of a peak in the first dimension of a comprehensive two-dimensional system, [2]t_R is the retention time of a peak in the second dimension, and [1]I is the retention index of a peak eluting from the first-dimension column. Nomenclature according to Wu et al. (2012). *Literature I and CAS number: the values were from the PubChem database and* NIST 2017. *MS identification based on* NIST 2017 *mass spectral database*

As can be seen, the PAC point had some samples with high peak intensities (orange to red colour), which was to be expected as this point is closer to sources of air pollution, such as a high volume of vehicle. However, some samples of the ECO point also presented high peak intensities, suggesting that atmospheric phenomena

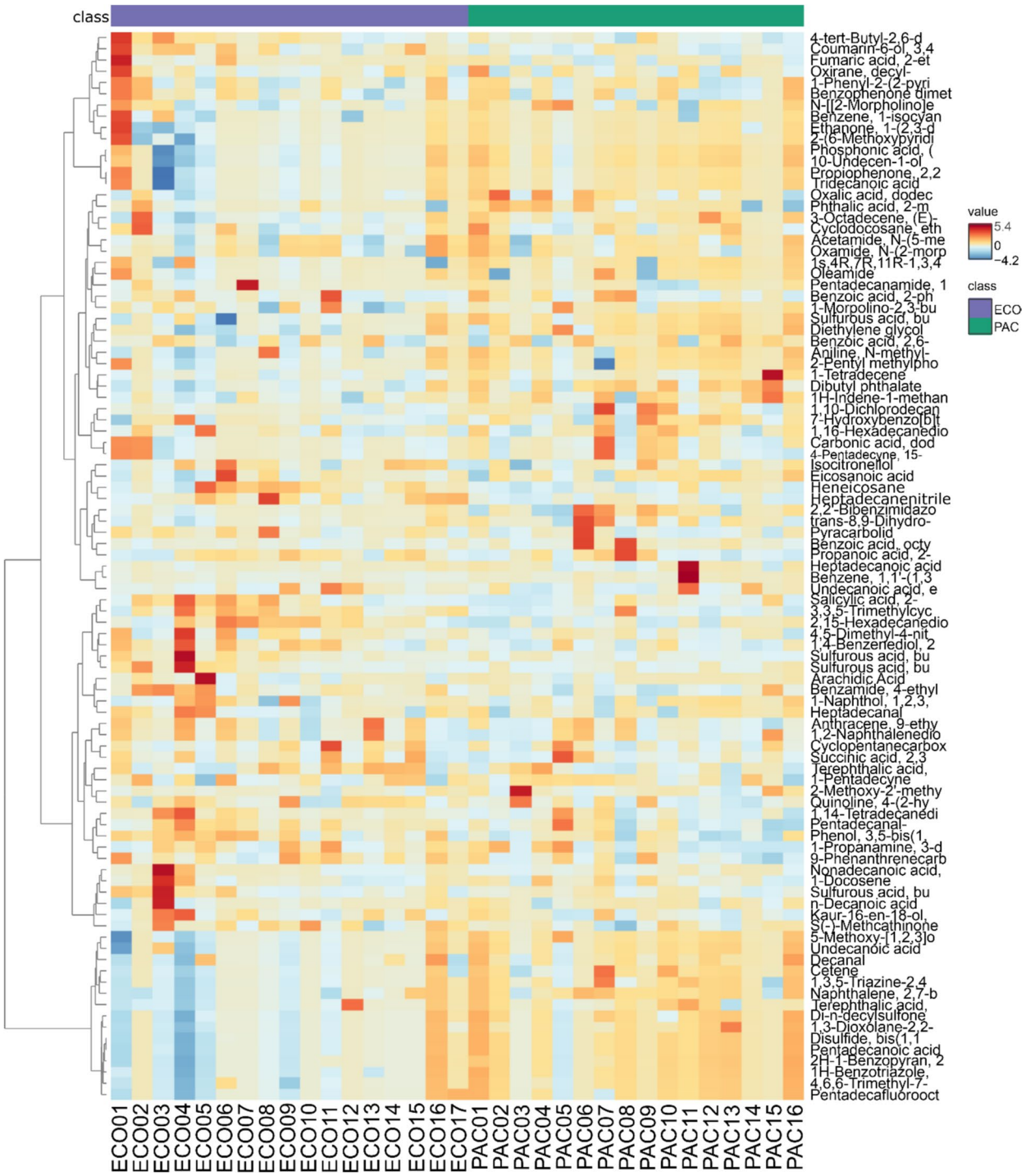

Fig. 3 Heatmap of the peak intensities of the most abundant compounds identified in $PM_{2.5}$ samples. ECO01 to ECO17 represent the filter samples of the ECO point; PAC01 to PAC16 represent the filter samples of the ECO point (the number after ECO and PAC is the sampling day)

contributed to the transport of pollutants from anthropogenic regions to the natural ambient ECO.

The compounds were divided into several chemical classes, as shown in Fig. 4. The largest class was aromatic compounds, which accounted for 29.2% of the total.

Among the leading representatives of this class, they stood out for their toxicity: PAH derivatives, aniline derivatives, and other aromatic compounds (Fig. 5).

PAHs are compounds formed during the incomplete combustion of organic material (pyrolysis). They are mainly

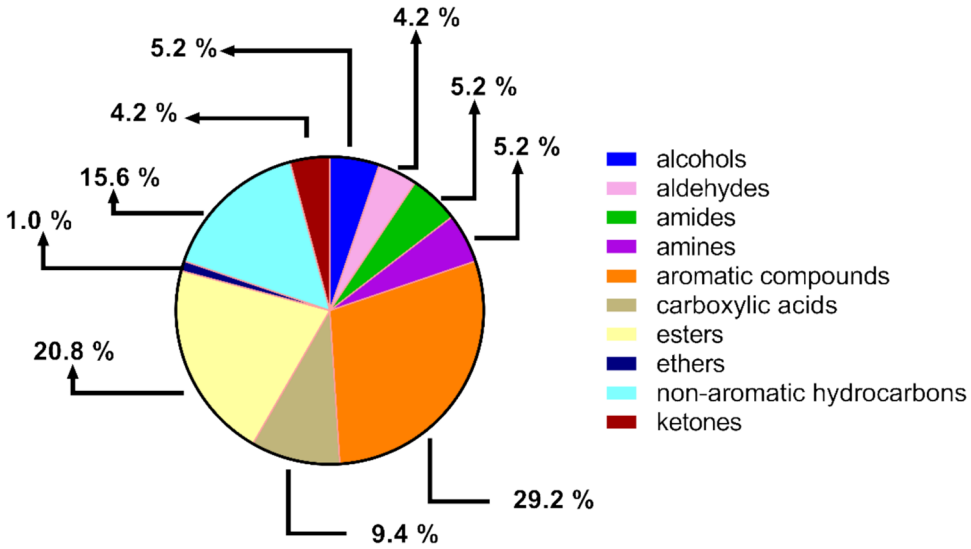

Fig. 4 Distribution by chemical class of compounds identified in $PM_{2.5}$ samples

emitted during the combustion of fossil fuels and anthropogenic activities (Buczyńska et al. 2013), but also from natural sources such as volcanic eruptions and accidental forest fires (Srogi 2007). PAH derivatives are referred to as OPAH (oxygenated PAH) and NPAH (nitrated PAH) and are formed in the atmosphere by reactions of PAH with hydroxyl radicals, nitrate, among others, and ozone or by photochemical processes (Andreou and Rapsomanikis 2009).

Some PAHs and their derivatives (such as benzo[*a*]pyrene and nitro-PAHs) have a carcinogenic/mutagenic effect on humans (Pedersen et al. 2004), and studies have already shown that derivatives are more toxic than PAHs (Albinet et al. 2008; Zhao et al. 2019; Ma et al. 2022). Of the derivatives identified in this study, the following were found in less than 3 days of sampling: 1*H*-phenanthro[9,10-*c*]pyrazole (PAC only); 2,2-diphenylchromene (PAC and ECO); 6-tridecyloxan-2-one (ECO only); 2,6-ditert-butyl-4-(2,6-ditert-butyl-4-methylpyran-4-yl)-4-methylpyran (PAC only); 9,10-dimethylanthracene (only PAC); 1-(2,3-dihydro-1*H*-inden-1-yl)ethanone (PAC and ECO); 2,4,5,7-tetramethylphenanthrene (only PAC) and 2-methylpyrene (only PAC). The others were identified in more than 3 days, and their distribution is shown in the box plots in Fig. 6. It is interesting to note that, except for 2,2-diphenylchromene, 9,10-dimethylanthracene, and 2-methylpyrene, the other compounds have not been reported to be detected in atmospheric PM, although they might have been detected previously. Derivatives, except for (8*S*,9*S*)−11-methyl-8,9-dihydrobenzo[*b*]phenanthrene-8,9-diol, were detected at both sampling points with no statistical difference between the PAC and ECO groups ($p > 0.05$). Although the ECO sampling point is a natural region, roads with high vehicle and factory traffic are nearby. Therefore, the identification of derivatives at the ECO point can also be explained by pollution from these anthropogenic sources. Identifying derivatives at the PAC point can be related to the sources of vehicle pollution characteristic of the avenue near this point.

In addition to compounds characteristic of anthropogenic activities, including caffeine, compounds of natural origin, known as biogenic semi-volatile compounds (BSVOCs), were also identified in the samples. Some of the identified BSVOCs were oleic acid, palmitoleic acid, stearic acid, vanillin acetate, isocitronellol, kaurenol, 1,14-tetradecanediol, 1,16-hexadecanediol, 10-undecen-1-ol, and n-tridecan-1-ol. As expected, most of these compounds were found in ECO, a dense forest region.

Some plasticisers were identified in the samples examined in this work, such as dibutyl phthalate, monomethyl phthalate, 2-methylbutylpentyester phthalic acid, isobutyl-2-pentylester phthalic acid, 2-ethylhexyl-octylester terephthalic acid, and 6-methylhept-2-yl-octylester terephthalic acid. These are esters derived from phthalic acid that are widely used in polymeric materials such as flooring, wallpaper, and food packaging and are also used in solvents, fragrances, repellents, shampoos, and other personal products (Afshari et al. 2004; Wang et al. 2018). Some of these compounds have endocrine effects in animals and humans and act as allergens (Marsee et al. 2006; Zhou et al. 2017, 2020).

Among the plasticisers identified in this study, dibutyl phthalate (DBP) is one of the most well-known because of its high toxicity. This compound was present in both the PAC and ECO samples. Fig. S4 shows that although the PAC samples had sampling days with higher peak intensity values for DBP, there was no statistical difference between the mean values of the samples ($p > 0.05$). The PAC site is more affected by pollution sources, as it has a high vehicle flow. It is also a region with a high concentration of buildings and residences that can release plasticisers from their components. These characteristics justify sampling days on which the DBP concentration in these samples is higher than

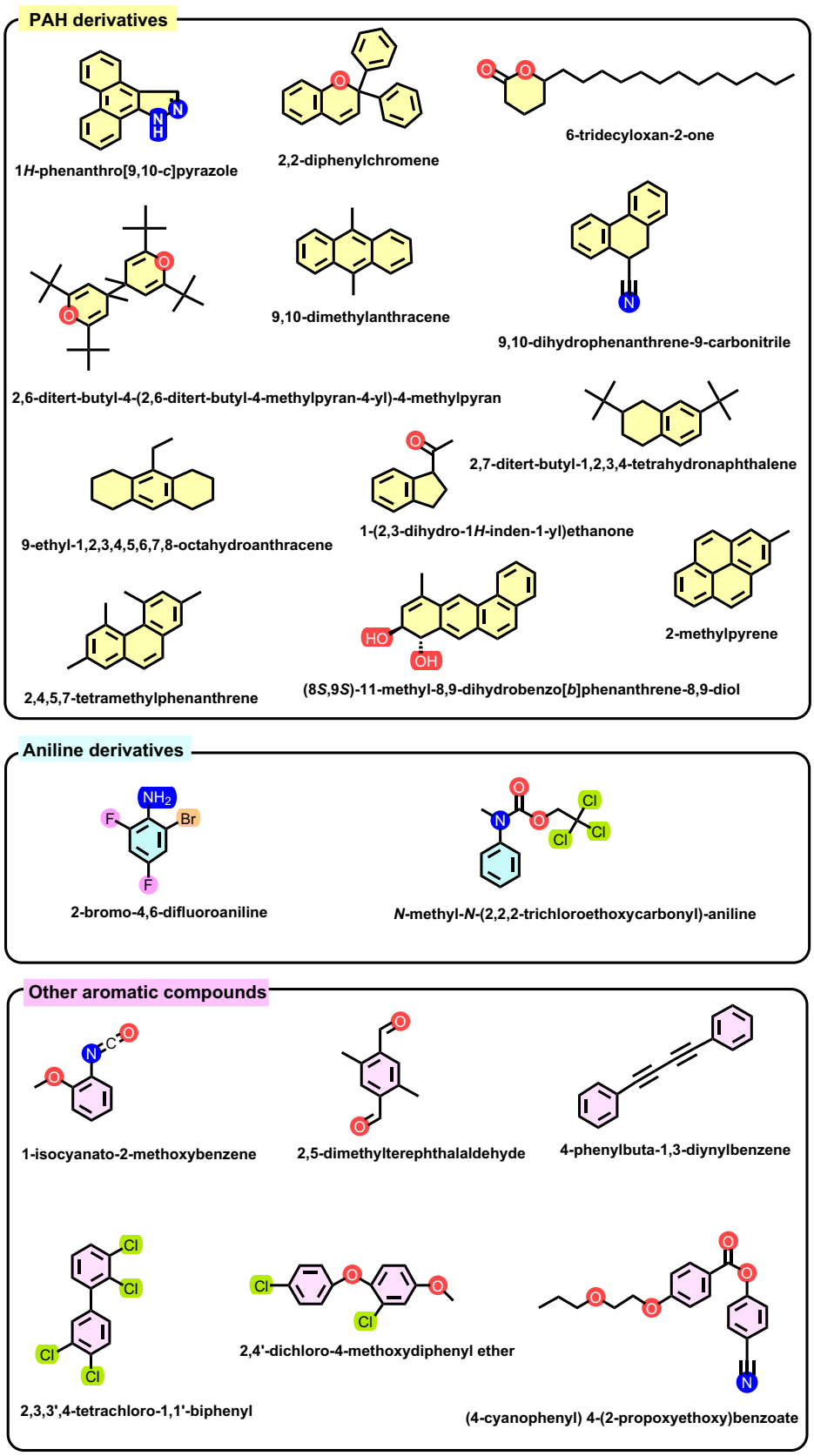

Fig. 5 Representative toxic compounds identified in $PM_{2.5}$ samples according to their chemical classes

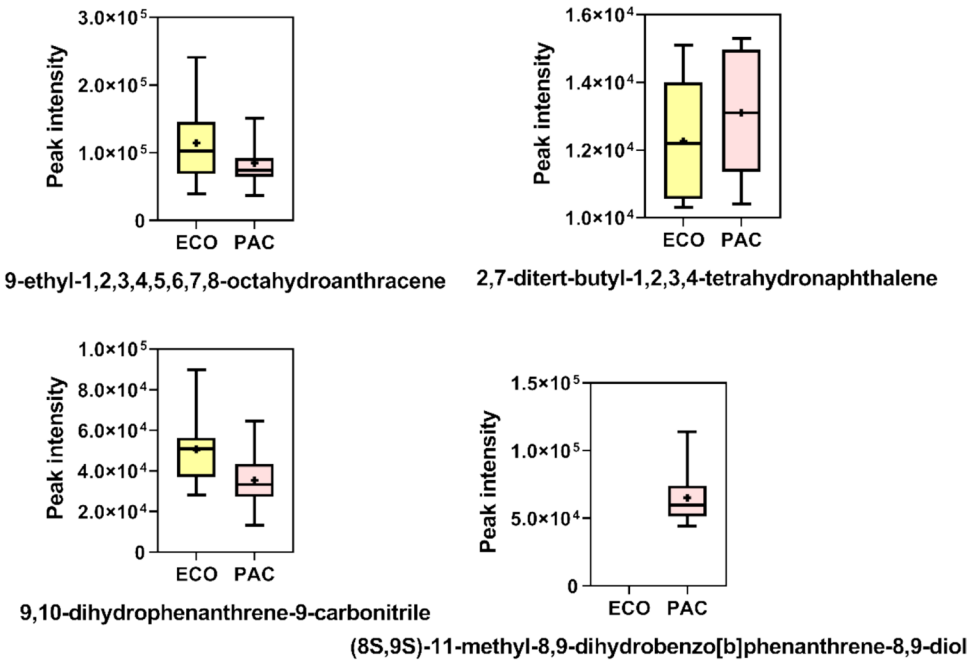

Fig. 6 Boxplots of some PAH derivatives identified in $PM_{2.5}$ samples (after outlier remotion). 9-ethyl-1,2,3,4,5,6,7,8-octahydroanthracene ($n = 16$ for ECO and $n = 15$ for PAC); 2,7-ditert-butyl-1,2,3,4-tetrahydronaphthalene ($n = 5$ for ECO and $n = 8$ for PAC); 9,10-dihydrophenanthrene-9-carbonitrile ($n = 17$ for ECO and $n = 16$ for PAC); (8S,9*S*)−11-methyl-8,9-dihydrobenzo[*b*]phenanthrene-8,9-diol ($n = 13$ for PAC)

in the sample from ECO. A non-sampled filter was analysed to exclude the background effect of phthalates, and no DBP was identified.

The peak intensities of the 189 compounds listed in Table 1 were used to build a PCA model. Four PCs were selected after analysing the eigenvalue curve. The constructed model captured 72.56% of the cumulative variance. PC 1 and PC 2 captured 52.02% of the total variance. The graph PC 1 × PC 2 is shown in Fig. 7A.

As can be seen in Fig. 7A, most of the samples of the PAC set were located on the negative side of PC 1, while the ECO samples were distributed mainly along the positive part of PC 1. This observation demonstrated a statistical difference between the two sets of samples. The loading plots (Fig. S5-A) can be used to determine which compounds are related to the separation observed in Fig. 7A. The charges on the right side of PC 1 are mainly associated with ECO samples that are responsible for the significant difference observed in PC 1. The main compounds that differentiate these samples in importance order are terephthalic acid, 6-methylhept-2-yl octyl ester; quinoline, 4-(2-hydroxy-2-methoxy-1-thioxoethyl)−2-phenyl-; 1-pentadecyne; and 2,15-hexadecanedione. These compounds chemically characterise the samples from ECO. The loadings related to the negative side of PC 1 were less critical for the PAC samples discrimination. The representative compounds were arachidic acid and benzoic acid, 2,6-dichloro, 2-acethylphenyl ester.

In the graph of PC 2 × PC 3 (Fig. 7B), it was observed that the pairs PAC07/PAC12 and PAC01/PAC04, on the negative side of PC 3 and ECO08/ECO10 on the positive side of PC 3 had very close scores, indicating a high similarity between these samples. On the other hand, in PC 1 × PC 3 (Fig. 8A), the ECO samples were distinguished by the first quadrant (formed by the positive sides of the PCs), and in PC 1 × PC 4 (Fig. 8B), the ECO samples were grouped in the second quadrant (positive side of PC 1 × negative side of PC 4). The proximity of the samples in each of these situations can be related to the similarity of climatic conditions and pollution levels on these sampling days, which allowed for similar profiles of the compounds in these samples. The proximity of the PAC and ECO samples is due to the fact that these samples had common compounds and likely similar weather conditions on the sample days. All these conclusions were drawn solely by visual inspection of the score plots. Since the PCA model is unsupervised, in other words, exploratory, the model cannot serve as a classification tool. For this, it would be necessary to create a supervised model, such as PLS-DA (partial least squares discriminant analysis), which requires a much higher number of samples than those collected in this work to construct the calibration and validation sets. However, the graphs of the PCA model provide exciting information about the behaviour of the samples.

The compounds with the highest loading values were selected for discussion. Thus, the top three compounds associated with the ECO samples were terephthalic acid, 6-methylhept-2-yl octyl ester; quinoline, 4-(2-hydroxy-2-methoxy-1-thioxoethyl)−2-phenyl- and 1-pentadecyne. Terephthalic acid, 6-methylhept-2-yl octyl ester is associated with plasticising materials and

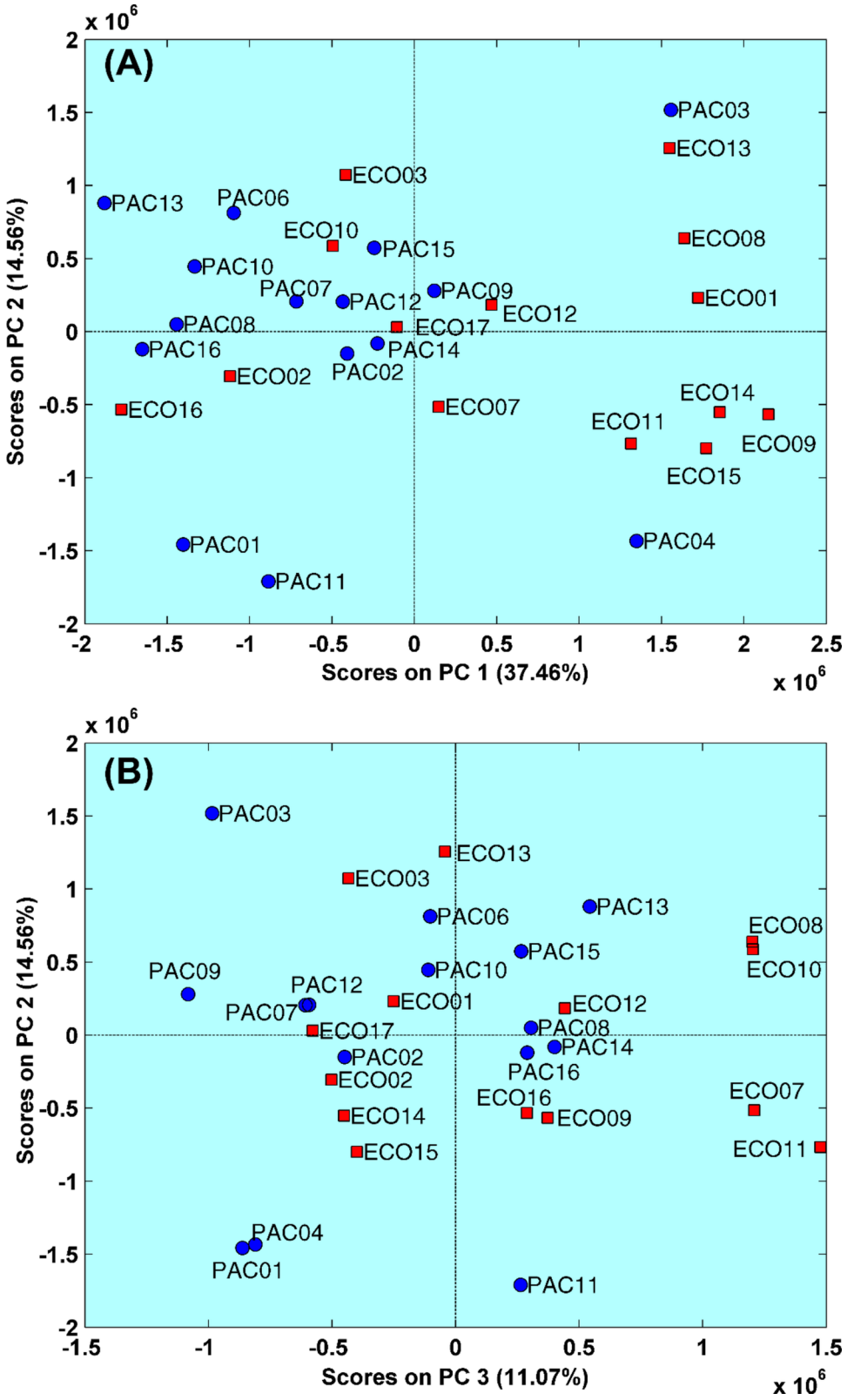

Fig. 7 Score plots of the PCA model. **A** PC 1 × PC 2; **B** PC 2 × PC 3. ECO (red), PAC (blue)

found in indoor dust samples (Pourasil et al. 2022). Although there have been no studies on the toxicity of this compound yet, some plasticisers represent toxicity of concern to humans, as mentioned earlier in this text. Quinoline derivatives, such as quinoline, 4-(2-hydroxy-2-methoxy-1-thioxoethyl)−2-phenyl-, are used as

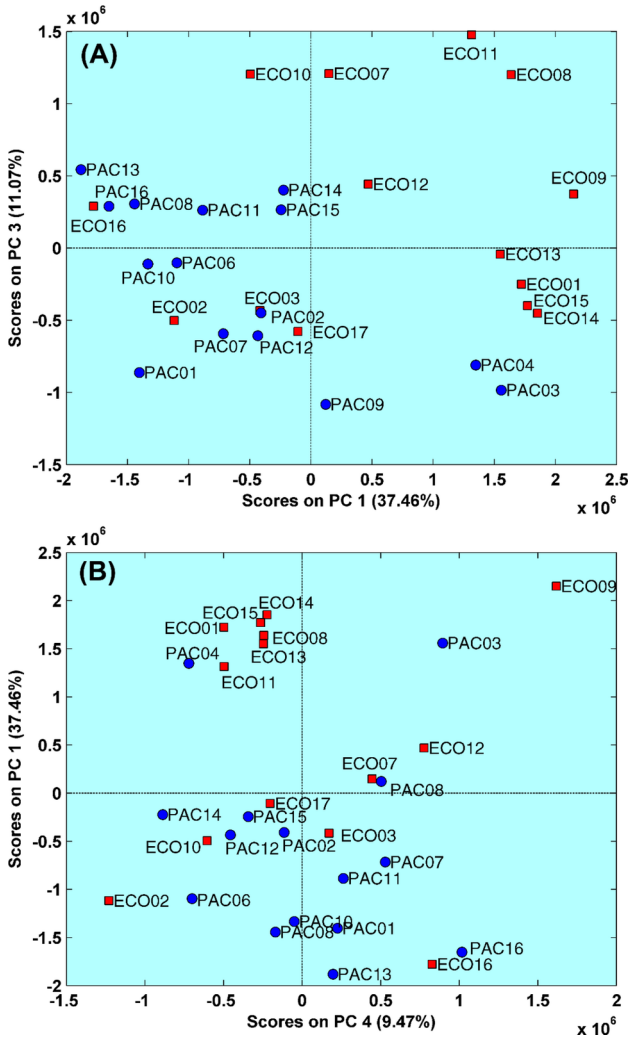

Fig. 8 Score plots of the PCA model. **A** PC 1×PC 3; **B** PC 1×PC 4. ECO (red), PAC (blue)

intermediates in polymer synthesis, and their emission into the air can occur from building materials (Pourasil et al. 2022). Hydrocarbons such as 1-pentadecyne, a long-chain alkyne, can be emitted from petrochemical sources, and the identification of this compound in samples can be linked to vehicle emissions from fossil fuel combustion (Feng et al. 2021). The unusual presence of these compounds in a natural region, such as ECO, could be related to the ubiquitous transport phenomena in the atmosphere, which are responsible for the relocation of pollutants from a polluted region to regions with low pollution or even to distant regions (Burkow and Kallenborn 2000; Tirabassi et al. 2020). ECO is surrounded by urban and industrial areas, which supports the hypothesis of atmospheric transport of pollutants.

The loading graph for the PAC samples showed that the compounds arachidic acid and benzoic acid, 2,6-dichloro-, 2-acethylphenyl ester were the most representative. Arachidic acid is a fatty acid found in plants and has already been found in the composition of biodiesel oil extracted from the seeds of the *Maesopsis eminii* tree (Joven et al. 2020). The compound also produces polymer films for electronic applications (Ren et al. 2005). Although PAC is in a region characterised mainly by high traffic volume and civil constructions, there is also a forest area near the sampling point. Therefore, the presence of arachidic acid may be related to natural emissions from the forested region or biodiesel vehicles. Compounds derived from benzoic acid, such as benzoic acid, 2,6-dichloro-, 2-acethylphenyl ester, are used as preservatives in the food industry and as food flavourings (Pourasil et al. 2022). The presence of this ester in the samples could be related to the food industries near the sampling points.

HS-GC/MS analysis

The HS-GC/MS analysis results differed from those obtained by DI-SPME-GC×GC/Q-TOFMS. Despite the high resolving power, sensitivity, and separability of GC×GC, the technique reached its limits in identifying certain compounds with higher volatility. However, these compounds could be effectively identified by HS-GC/MS. This limitation could be due to the extraction method used in the sample preparation, particularly the direct immersion mode with SPME and the extraction temperature. These favourable characteristics include the removal of more volatile compounds in the headspace and the extraction of semi-volatile compounds in an aqueous medium. In this respect, analysis with HS-SPME and DI-SPME could allow a more detailed identification of SVOCs/VOCs.

Table 2 shows the VOCs determined with the validated analytical method of HS-GC/MS. Most compounds can be attributed to PAC samples collected in a high-traffic environment (Fig. 9). However, ECO samples collected in a greener environment showed a significant decrease in the identification and concentrations of these VOCs. Although vehicle traffic is lower at this sampling site, vegetation can also influence VOC levels in the air. In this regard, recent studies have shown that certain plants promote the absorption/breakdown of VOCs (Brilli et al. 2018; Bandehali et al. 2021; Shen et al. 2024).

BTEX (benzene, toluene, ethylbenzene, and xylenes) had the highest concentration in the collected samples at the PAC sampling site. It should be noted that these types of aromatic compounds are analysed directly in the gas phase of the air due to their higher presence, while $PM_{2.5}$ is used more for the analysis of SVOCs (dos Santos et al. 2020) and heavy metals (Idris et al. 2020). As a result, detailed studies on BTEX in $PM_{2.5}$ are not found in the literature, and

Table 2 VOCs found in the collected samples using HS-GC/MS

N°	VOCs	Average concentration (ng m^{-3})*			
		ECO	Positive samples	PAC	Positive samples
1	Methylene chloride	<LOD	-	0.27	5
2	Bromochloromethane	<LOD	-	0.32	3
3	Chloroform	<LOD	-	0.31	5
4	Benzene	1.35	5	10.61	12
5	Toluene	0.89	4	8.09	12
6	Chlorobenzene	<LOD	-	0.43	6
7	1,1,1,2-tetrachloroethane	<LOD	-	0.39	3
8	Ethylbenzene	0.33	4	10.25	13
9	P-xylene/M-xylene	1,29	4	11.80	12
11	O-xylene	0.79	4	9.34	13
12	Styrene	<LOQ	3	1.67	12
13	Bromobenzene	<LOQ	-	0.56	4
14	N-propylbenzene	<LOD	-	0.43	4
15	1,3,5-trimethylbenzene	<LOD	-	0.32	5
16	1,2,4-trimethylbenzene	<LOD	-	0.38	6
17	1,3-dichlorobenzene	<LOD	-	<LOQ	-
18	1,4-dichlorobenzene	<LOD	-	<LOQ	-
19	1,3,5-trichlorobenzene	<LOD	-	<LOQ	-
20	1,2,4-trichlorobenzene	<LOD	-	<LOQ	-
21	Naphthalene	0.18	2	0.65	4

**Calculated based on the mass (ng) of the analyte bound to $PM_{2.5}$ on the quartz filter and the volume (m^3) of air sampled, measured at 25 °C and 1 atm of pressure*

comparisons with maximum contaminant levels (MCL) of environmental agencies would fail. However, this type of analysis contributes to studies on exposure to mostly volatile compounds.

Conclusions

The use of GC×GC/Q-TOFMS in combination with DI-SPME extraction and the application of DoE and RSM in the optimisation of parameters related to the thermal modulation process proved to be efficient in the analysis of VOCs/ SVOCs in $PM_{2.5}$ samples. DoE/RSM saved time developing the chromatographic method by reducing the number of experiments required to achieve optimal two-dimensional separation conditions. Compounds of different chemical classes were found in the samples, which focused on contaminants with high toxicity to humans, such as some PAH derivatives, plasticisers, and other aromatic compounds. Some of these compounds had not been previously identified in particulate matter, and no studies on their toxicity are in the relevant literature. This work identifies previously unreported compounds in PM samples, offering valuable data to support future toxicological studies on human exposure to these air pollutants. Furthermore, HS-GC/MS also led to the identification of other compounds with high volatility.

Fig. 9 Satellite image indicating the PM sampling points (approximately 1.8 km between points)

Supplementary Information The online version contains supplementary material available at https://doi.org/10.1007/s11356-024-35647-y.

Author contribution All authors contributed to the conception and design of the study. The formal analysis, validation, methodology, data collection, and original draught writing were performed by Josimar M. Batista and Eduard F. Valenzuela. Helvécio C. Menezes conducted conceptualisation, review, and editing. Zenilda L. Cardeal performed conceptualisation, methodology, review, editing, and supervision. All authors commented on previous versions of the manuscript, and all authors read and approved the final manuscript.

Funding The authors are grateful to the funding received from Conselho Nacional de Desenvolvimento Científico e Tecnológico (CNPq), Coordenação de Aperfeiçoamento de Pessoal de Nível Superior (CAPES) and Fundação de Amparo à Pesquisa de Minas Gerais (FAPEMIG).

Data availability All data and materials are available upon journal request.

Declarations

Ethical approval Not applicable.

Consent to participate All authors consented to participate in the draughting of this research article.

Consent for publication All authors consented to publish this research article.

Competing interests The authors declare no competing interests.

References

Afshari A, Gunnarsen L, Clausen PA, Hansen V (2004) Emission of phthalates from PVC and other materials. Indoor Air 14:120–128. https://doi.org/10.1046/j.1600-0668.2003.00220.x

Albinet A, Leoz-Garziandia E, Budzinski H et al (2008) Nitrated and oxygenated derivatives of polycyclic aromatic hydrocarbons in the ambient air of two French alpine valleys. Part 1: Concentrations, sources and gas/particle partitioning. Atmos Environ 42:43–54. https://doi.org/10.1016/j.atmosenv.2007.10.009

Andreou G, Rapsomanikis S (2009) Polycyclic aromatic hydrocarbons and their oxygenated derivatives in the urban atmosphere of Athens. J Hazard Mater 172:363–373. https://doi.org/10.1016/j.jhazmat.2009.07.023

Bandehali S, Miri T, Onyeaka H, Kumar P (2021) Current state of indoor air phytoremediation using potted plants and green walls. Atmosphere (Basel) 12:473. https://doi.org/10.3390/atmos12040473

Bhatt K, Dejong T, Dubois LM et al (2022) Lipid serum profiling of boar-tainted and untainted pigs using GC×GC–TOFMS: an exploratory study. Metabolites 12:0–9. https://doi.org/10.3390/metabo12111111

Boegelsack N, Hayes K, Sandau C et al (2021) Method development for optimizing analysis of ignitable liquid residues using flow-modulated comprehensive two-dimensional gas chromatography. J Chromatogr A 1656:462495. https://doi.org/10.1016/j.chroma.2021.462495

Brilli F, Fares S, Ghirardo A et al (2018) Plants for sustainable improvement of indoor air quality. Trends Plant Sci 23:507–512. https://doi.org/10.1016/j.tplants.2018.03.004

Buczyńska AJ, Geypens B, Van Grieken R, De Wael K (2013) Stable carbon isotopic ratio measurement of polycyclic aromatic hydrocarbons as a tool for source identification and apportionment—a review of analytical methodologies. Talanta 105:435–450. https://doi.org/10.1016/j.talanta.2012.10.075

Burkow IC, Kallenborn R (2000) Sources and transport of persistent pollutants to the Arctic. Toxicol Lett 112–113:87–92. https://doi.org/10.1016/S0378-4274(99)00254-4

Cardador MJ, Gallego M (2017) Simultaneous determination of 14 disinfection by-products in meat products using microwave-assisted extraction and static headspace coupled to gas chromatography–mass spectrometry. J Chromatogr A 1509:9–15. https://doi.org/10.1016/j.chroma.2017.06.028

Cerqueira UMFM, Bezerra MA, Ferreira SLC et al (2021) Doehlert design in the optimization of procedures aiming food analysis – a review. Food Chem 364:130429. https://doi.org/10.1016/j.foodchem.2021.130429

Cheong KW, Tan CP, Mirhosseini H et al (2011) Optimization of equilibrium headspace analysis of volatile flavor compounds of malaysian soursop (Annona muricata): Comprehensive two-dimensional gas chromatography time-of-flight mass spectrometry (GC×GC-TOFMS). Food Chem 125:1481–1489. https://doi.org/10.1016/j.foodchem.2010.10.067

Dai L-W, Meng J, Li Q-Q et al (2021) VOCs Emission inventory and variation characteristics of artificial sources in Hubei Province in the Yangtze River Economic Belt. Huan Jing Ke Xue 42:1039–1052. https://doi.org/10.13227/j.hjkx.202009043

Delove Tegladza I, Qi T, Chen T et al (2020) Direct immersion single-drop microextraction of semi-volatile organic compounds in environmental samples: a review. J Hazard Mater 393:122403. https://doi.org/10.1016/j.jhazmat.2020.122403

dos Santos RR, de Cardeal Z, L, Menezes HC, (2020) Phase distribution of polycyclic aromatic hydrocarbons and their oxygenated and nitrated derivatives in the ambient air of a Brazilian urban area. Chemosphere 250:126223. https://doi.org/10.1016/j.chemosphere.2020.126223

Drabińska N, Jeleń HH (2022) Optimisation of headspace solid-phase microextraction with comprehensive two-dimensional gas chromatography–time of flight mass spectrometry (HS-SPME–GC × GC–ToFMS) for quantitative analysis of volatile compounds in vegetable oils using statistical experi. J Food Compos Anal 110:104595. https://doi.org/10.1016/j.jfca.2022.104595

EPA (2024) Technical overview of volatile organic compounds. https://www.epa.gov/indoor-air-quality-iaq/technical-overview-volatile-organic-compounds. Accessed 15 Jun 2024

Evagelopoulos V, Charisiou ND, Zoras S (2022) Dataset of polycyclic aromatic hydrocarbons and trace elements in PM2.5 and PM10 atmospheric particles from two locations in North-Western Greece. Data Br 42:108266. https://doi.org/10.1016/j.dib.2022.108266

Feng M, Hu X, Zhou L et al (2021) Real-world vehicle volatile organic compound emissions and their source profile in Chengdu based on a roadside and tunnel study. Atmosphere (Basel) 12:861. https://doi.org/10.3390/atmos12070861

Gaines RB (1998) Characterization of petroleum-based fuels using comprehensive two-dimensional gas chromatography. Dissertation, University of Connecticut. https://digitalcommons.lib.uconn.edu/dissertations/AAI9909784

Gerster FM, Vernez D, Wild PP, Hopf NB (2014) Hazardous substances in frequently used professional cleaning products. Int J Occup Environ Health 20(1):46–60. https://doi.org/10.1179/2049396713Y.0000000052

Guan W-J, Zheng X-Y, Chung KF, Zhong N-S (2016) Impact of air pollution on the burden of chronic respiratory diseases in China: time for urgent action. Lancet 388:1939–1951. https://doi.org/10.1016/S0140-6736(16)31597-5

Idris SA 'Ainaa,' Hanafiah MM, Khan MF, Hamid HHA (2020) Indoor generated PM2.5 compositions and volatile organic compounds: potential sources and health risk implications. Chemosphere 255:126932. https://doi.org/10.1016/j.chemosphere.2020.126932

Ieda T, Hashimoto S (2023) GC × GC and computational strategies for detecting and analyzing environmental contaminants. TrAC Trends Anal Chem 165:117118. https://doi.org/10.1016/j.trac.2023.117118

Jalili V, Barkhordari A, Norouzian Baghani A (2019) The role of microextraction techniques in occupational exposure assessment. A Review Microchem J 150:104086. https://doi.org/10.1016/j.microc.2019.104086

Jeong G-Y, Kim J-H, Hong Y et al (2024) Volatile organic compounds sampling and analysis using needle trap device. J Chromatogr Open 5:100112. https://doi.org/10.1016/j.jcoa.2023.100112

Joven JMO, Gadian JT, Perez MA et al (2020) Optimized ultrasonic-assisted oil extraction and biodiesel production from the seeds of Maesopsis eminii. Ind Crops Prod 155:112772. https://doi.org/10.1016/j.indcrop.2020.112772

Kaikiti C, Stylianou M, Agapiou A (2022) TD-GC/MS analysis of indoor air pollutants (VOCs, PM) in hair salons. Chemosphere 294:133691. https://doi.org/10.1016/j.chemosphere.2022.133691

Kakavandi B, Rafiemanesh H, Giannakis S et al (2023) Establishing the relationship between Polycyclic Aromatic Hydrocarbons (PAHs) exposure and male infertility: a systematic review. Ecotoxicol Environ Saf 250:114485. https://doi.org/10.1016/j.ecoenv.2022.114485

Kulsing C, Nolvachai Y, Marriott PJ (2020) Concepts, selectivity options and experimental design approaches in multidimensional and comprehensive two-dimensional gas chromatography. TrAC Trends Anal Chem 130:115995. https://doi.org/10.1016/j.trac.2020.115995

León VM, Llorca-Pórcel J, Álvarez B et al (2006) Analysis of 35 priority semi-volatile compounds in water by stir bar sorptive extraction–thermal desorption–gas chromatography–mass spectrometry. Anal Chim Acta 558:261–266. https://doi.org/10.1016/j.aca.2005.10.080

Li Y-W, Ma W-L (2021) Photocatalytic oxidation technology for indoor air pollutants elimination: a review. Chemosphere 280:130667. https://doi.org/10.1016/j.chemosphere.2021.130667

Li J-R, Wang F-K, He C et al (2020) Catalytic total oxidation of toluene over carbon-supported Cu Co oxide catalysts derived from Cu-based metal organic framework. Powder Technol 363:95–106. https://doi.org/10.1016/j.powtec.2019.12.060

Li N, Zhang H, Zhu S et al (2023) Secondary PM2.5 dominates aerosol pollution in the Yangtze River Delta region: environmental and health effects of the Clean air Plan. Environ Int 171:107725. https://doi.org/10.1016/j.envint.2022.107725

Lim YM, Swamy V, Ramakrishnan N et al (2023) Volatile organic compounds (VOCs) in wastewater: recent advances in detection and quantification. Microchem J 195:109537. https://doi.org/10.1016/j.microc.2023.109537

Liu X, Hu Q, Tong Y et al (2021) Sample bottle coated with sorbent as a novel solid-phase extraction device for rapid on-site detection of BTEX in water. Anal Chim Acta 1152:338226. https://doi.org/10.1016/j.aca.2021.338226

Lyu X, Guo H, Wang Y et al (2020) Hazardous volatile organic compounds in ambient air of China. Chemosphere 246:125731. https://doi.org/10.1016/j.chemosphere.2019.125731

Ma S, Chen H, Yue C et al (2022) Atmospheric occurrences of nitrated and hydroxylated polycyclic aromatic hydrocarbons from typical e-waste dismantling sites. Environ Pollut 308:119713. https://doi.org/10.1016/j.envpol.2022.119713

Maceira A, Marcé RM, Borrull F (2020) Analytical methods for determining organic compounds present in the particulate matter from outdoor air. TrAC Trends Anal Chem 122:115707. https://doi.org/10.1016/j.trac.2019.115707

Marsee K, Woodruff TJ, Axelrad DA et al (2006) Estimated daily phthalate exposures in a population of mothers of male infants exhibiting reduced anogenital distance. Environ Health Perspect 114:805–809. https://doi.org/10.1289/EHP.8663/ASSET/A1D2ECCA-8F44-4DAA-B9C7-C794DBB80452/ASSETS/GRAPHIC/EHP0114-000805E4.JPG

Martínez A, Hernández A, Moraga C et al (2022) Detection of volatile organic compounds associated with mechanical damage in apple cv. 'Golden Delicious' by headspace solid-phase microextraction (HS-SPME) and GC-MS analysis. LWT 172:114213. https://doi.org/10.1016/j.lwt.2022.114213

Moser B, Steininger-Mairinger T, Jandric Z et al (2023) Spoilage markers for freshwater fish: a comprehensive workflow for non-targeted analysis of VOCs using DHS-GC-HRMS. Food Res Int 172:113123. https://doi.org/10.1016/j.foodres.2023.113123

Murillo JH, Villalobos MC, Rojas Marín JF et al (2017) Polycyclic aromatic hydrocarbons in PM2.5 and PM10 atmospheric particles in the Metropolitan Area of Costa Rica: sources, temporal and spatial variations. Atmos Pollut Res 8:320–327. https://doi.org/10.1016/j.apr.2016.10.002

Murrell KA, Dorman FL (2021) A comparison of liquid-liquid extraction and stir bar sorptive extraction for multiclass organic contaminants in wastewater by comprehensive two-dimensional gas chromatography time of flight mass spectrometry. Talanta 221:121481. https://doi.org/10.1016/j.talanta.2020.121481

Nie J, Teng Y-J, Li Z-G et al (2016) Magnetic nanoparticles used in headspace extraction coupled with DSI-GC-IT/MS for analysis of VOCs in dry Traditional Chinese Medicine. Chinese Chem Lett 27:178–184. https://doi.org/10.1016/j.cclet.2015.09.006

NIST (2017) NIST chemistry web book. In: Natl. Inst. Stand. Technol. https://webbook.nist.gov/chemistry/. Accessed 16 Jan 2024

Pathak AK, Viphavakit C (2022) A review on all-optical fiber-based VOC sensors: heading towards the development of promising technology. Sensors Actuators A Phys 338:113455. https://doi.org/10.1016/j.sna.2022.113455

Pedersen DU, Durant JL, Penman BW et al (2004) Human-cell mutagens in respirable airborne particles in the Northeastern United States. 1. Mutagenicity of fractionated samples. Environ Sci Technol 38:682–689. https://doi.org/10.1021/es0347282

Pourasil RSM, Cristale J, Lacorte S, Tauler R (2022) Non-targeted Gas Chromatography Orbitrap Mass Spectrometry qualitative and quantitative analysis of semi-volatile organic compounds in indoor dust using the Regions of Interest Multivariate Curve Resolution chemometrics procedure. J Chromatogr A 1668:462907. https://doi.org/10.1016/j.chroma.2022.462907

Ren L, Kang SZ, Zhang HM et al (2005) Investigation of ITO surface modified by NPB and arachidic acid LB films. Colloids Surfaces A Physicochem Eng Asp 257–258:433–437. https://doi.org/10.1016/j.colsurfa.2004.10.097

Salvador ÂC, Baptista I, Barros AS et al (2013) Can volatile organic metabolites be used to simultaneously assess microbial and mite contamination level in cereal grains and coffee beans? PLoS One 8:e59338. https://doi.org/10.1371/journal.pone.0059338

Sarafraz-Yazdi A, Amiri AH, Es'haghi Z (2008) BTEX determination in water matrices using HF-LPME with gas chromatography–flame ionization detector. Chemosphere 71:671–676. https://doi.org/10.1016/j.chemosphere.2007.10.073

Schmekel B, Winquist F, Vikström A (2014) Analysis of breath samples for lung cancer survival. Anal Chim Acta 840:82–86. https://doi.org/10.1016/j.aca.2014.05.034

Setyaningsih W, Majchrzak T, Dymerski T et al (2019) Key-marker volatile compounds in aromatic rice (Oryza sativa) grains: an

HS-SPME extraction method combined with GC×GC-TOFMS. Molecules 24:4180. https://doi.org/10.3390/molecules24224180
Shen X, Sun Q, Mosey G et al (2024) Benchmark of plant-based VOCs control effect for indoor air quality: green wall case in smith campus at Harvard University. Sci Total Environ 906:166269. https://doi.org/10.1016/j.scitotenv.2023.166269
Skartland LK, Mjøs SA, Grung B (2011) Experimental designs for modeling retention patterns and separation efficiency in analysis of fatty acid methyl esters by gas chromatography–mass spectrometry. J Chromatogr A 1218:6823–6831. https://doi.org/10.1016/j.chroma.2011.07.077
Snow NH (2020) Basic multidimensional gas chromatography, 1st edn. Separation Science and Technology, London
Srogi K (2007) Monitoring of environmental exposure to polycyclic aromatic hydrocarbons: a review. Environ Chem Lett 5:169–195. https://doi.org/10.1007/s10311-007-0095-0
Stefanuto PH, Perrault KA, Dubois LM et al (2017) Advanced method optimization for volatile aroma profiling of beer using two-dimensional gas chromatography time-of-flight mass spectrometry. J Chromatogr A 1507:45–52. https://doi.org/10.1016/j.chroma.2017.05.064
Tirabassi T, Costa CP, Rui K (2020) Influence of dry deposition velocity to the ground in the dispersion of the air pollutants. IOP Conf Ser Earth Environ Sci 489:012003. https://doi.org/10.1088/1755-1315/489/1/012003
Valenzuela EF, de Paula FGF, Teixeira APC et al (2020) A new carbon nanomaterial solid-phase microextraction to pre-concentrate and extract pesticides in environmental water. Talanta 217:121011. https://doi.org/10.1016/j.talanta.2020.121011
van Den Dool H, Dec Kratz P (1963) A generalization of the retention index system including linear temperature programmed gas—liquid partition chromatography. J Chromatogr A 11:463–471. https://doi.org/10.1016/S0021-9673(01)80947-X
Vyviurska O, Koljančić N, Gomes AA, Špánik I (2022) Optimization of enantiomer separation in flow-modulated comprehensive two-dimensional gas chromatography by response surface methodology coupled to artificial neural networks: wine analysis case study. J Chromatogr A 1675:463189. https://doi.org/10.1016/j.chroma.2022.463189
Wang XD, Su GY, Zhao C et al (2018) Anticancer activity and potential mechanisms of 1C, a ginseng saponin derivative, on prostate cancer cells. J Ginseng Res 42:133–143. https://doi.org/10.1016/j.jgr.2016.12.014
Wang Z, Wei W, Zheng F (2020) Effects of industrial air pollution on the technical efficiency of agricultural production: evidence from China. Environ Impact Assess Rev 83:106407. https://doi.org/10.1016/j.eiar.2020.106407
Yang D-L, Zhang Z-N, Liu H et al (2023) Indoor air pollution and human ocular diseases: associated contaminants and underlying pathological mechanisms. Chemosphere 311:137037. https://doi.org/10.1016/j.chemosphere.2022.137037
Zhao J, Zhang Y, Wang T et al (2019) Characterization of PM2.5-bound polycyclic aromatic hydrocarbons and their derivatives (nitro-and oxy-PAHs) emissions from two ship engines under different operating conditions. Chemosphere 225:43–52. https://doi.org/10.1016/j.chemosphere.2019.03.022
Zhou C, Gao L, Flaws JA (2017) Prenatal exposure to an environmentally relevant phthalate mixture disrupts reproduction in F1 female mice. Toxicol Appl Pharmacol 318:49–57. https://doi.org/10.1016/J.TAAP.2017.01.010
Zhou S, Han M, Ren Y et al (2020) Dibutyl phthalate aggravated asthma-like symptoms through oxidative stress and increasing calcitonin gene-related peptide release. Ecotoxicol Environ Saf 199:110740. https://doi.org/10.1016/J.ECOENV.2020.110740
Zhu L, Shen D, Luo KH (2020) A critical review on VOCs adsorption by different porous materials: species, mechanisms and modification methods. J Hazard Mater 389:122102. https://doi.org/10.1016/j.jhazmat.2020.122102
Zou Y, Stefanuto PH, Maimone M et al (2021) Unraveling the complex olefin isomer mixture using two-dimensional gas chromatography-photoionization-time of flight mass spectrometry. J Chromatogr A 1645:462103. https://doi.org/10.1016/j.chroma.2021.462103

Terms and Conditions

Springer Nature journal content, brought to you courtesy of Springer Nature Customer Service Center GmbH (“Springer Nature”).
Springer Nature supports a reasonable amount of sharing of research papers by authors, subscribers and authorised users (“Users”), for small-scale personal, non-commercial use provided that all copyright, trade and service marks and other proprietary notices are maintained. By accessing, sharing, receiving or otherwise using the Springer Nature journal content you agree to these terms of use (“Terms”). For these purposes, Springer Nature considers academic use (by researchers and students) to be non-commercial.
These Terms are supplementary and will apply in addition to any applicable website terms and conditions, a relevant site licence or a personal subscription. These Terms will prevail over any conflict or ambiguity with regards to the relevant terms, a site licence or a personal subscription (to the extent of the conflict or ambiguity only). For Creative Commons-licensed articles, the terms of the Creative Commons license used will apply.
We collect and use personal data to provide access to the Springer Nature journal content. We may also use these personal data internally within ResearchGate and Springer Nature and as agreed share it, in an anonymised way, for purposes of tracking, analysis and reporting. We will not otherwise disclose your personal data outside the ResearchGate or the Springer Nature group of companies unless we have your permission as detailed in the Privacy Policy.
While Users may use the Springer Nature journal content for small scale, personal non-commercial use, it is important to note that Users may not:

1. use such content for the purpose of providing other users with access on a regular or large scale basis or as a means to circumvent access control;
2. use such content where to do so would be considered a criminal or statutory offence in any jurisdiction, or gives rise to civil liability, or is otherwise unlawful;
3. falsely or misleadingly imply or suggest endorsement, approval , sponsorship, or association unless explicitly agreed to by Springer Nature in writing;
4. use bots or other automated methods to access the content or redirect messages
5. override any security feature or exclusionary protocol; or
6. share the content in order to create substitute for Springer Nature products or services or a systematic database of Springer Nature journal content.

In line with the restriction against commercial use, Springer Nature does not permit the creation of a product or service that creates revenue, royalties, rent or income from our content or its inclusion as part of a paid for service or for other commercial gain. Springer Nature journal content cannot be used for inter-library loans and librarians may not upload Springer Nature journal content on a large scale into their, or any other, institutional repository.
These terms of use are reviewed regularly and may be amended at any time. Springer Nature is not obligated to publish any information or content on this website and may remove it or features or functionality at our sole discretion, at any time with or without notice. Springer Nature may revoke this licence to you at any time and remove access to any copies of the Springer Nature journal content which have been saved.
To the fullest extent permitted by law, Springer Nature makes no warranties, representations or guarantees to Users, either express or implied with respect to the Springer nature journal content and all parties disclaim and waive any implied warranties or warranties imposed by law, including merchantability or fitness for any particular purpose.
Please note that these rights do not automatically extend to content, data or other material published by Springer Nature that may be licensed from third parties.
If you would like to use or distribute our Springer Nature journal content to a wider audience or on a regular basis or in any other manner not expressly permitted by these Terms, please contact Springer Nature at

onlineservice@springernature.com